

# Heterogeneous Multi-Agent Proximal Policy Optimization for Power Distribution System Restoration

1<sup>st</sup> Parya Dolatyabi

*Department of Computer Science  
University of Tulsa  
Tulsa, USA  
parya-dolatyabi@utulsa.edu*

2<sup>nd</sup> Ali Farajzadeh Bavil

*Department of Computer Science  
University of Tulsa  
Tulsa, USA  
ali-farajzadeh@utulsa.edu*

3<sup>rd</sup> Mahdi Khodayar

*Department of Computer Science  
University of Tulsa  
Tulsa, USA  
mahdi-khodayar@utulsa.edu*

**Abstract**—Restoring power distribution systems (PDS) after large-scale outages requires sequential switching operations that reconfigure feeder topology and coordinate distributed energy resources (DERs) under nonlinear constraints such as power balance, voltage limits, and thermal ratings. These challenges make conventional optimization and value-based RL approaches computationally inefficient and difficult to scale. This paper applies a Heterogeneous-Agent Reinforcement Learning (HARL) framework—instantiated through Heterogeneous-Agent Proximal Policy Optimization (HAPPO)—to enable coordinated restoration across interconnected microgrids. Each agent controls a distinct microgrid with different loads, DER capacities, and switch counts, introducing practical structural heterogeneity. Decentralized actor policies are trained with a centralized critic to compute advantage values for stable on-policy updates. A physics-informed OpenDSS environment provides full power-flow feedback and enforces operational limits via differentiable penalty signals rather than invalid action masking. The total DER generation is capped at 2400 kW, and each microgrid must satisfy local supply–demand feasibility. Experiments on the IEEE 123-bus and IEEE 8500-node systems show that HAPPO achieves faster convergence, higher restored power, and smoother multi-seed training than DQN, PPO, MAES, MAGDPG, MADQN, Mean-Field RL, and QMIX. Results demonstrate that incorporating microgrid-level heterogeneity within the HARL framework yields a scalable, stable, and constraint-aware solution for complex PDS restoration.

**Index Terms**—Power system restoration, Reinforcement learning, Heterogeneous-Agent Proximal Policy Optimization.

## I. INTRODUCTION

Modern power distribution systems face increasing exposure to environmental hazards, component aging, and cybersecurity threats, resulting in frequent service interruptions [1]. Distributed energy resources (DERs) such as photovoltaics, microturbines, and storage can accelerate local recovery [2], yet their limited capacity and the voltage, thermal, and topological constraints of distribution feeders complicate safe and efficient restoration [3]. Recent advancements in machine

This research is supported by the National Science Foundation (NSF) under grant ECCS-2223628.

learning for critical infrastructure highlight the growing role of data-driven recovery, including a transformer–reinforcement learning framework for large-scale repair sequencing that enables faster and more resilient system restoration [4]. Machine learning has also advanced modeling in other safety-critical physical domains, including high-fidelity ground-motion prediction using ensemble techniques [5].

Conventional restoration is typically formulated as a mixed-integer nonlinear optimization problem [6]–[8], which may provide optimal switching plans but requires accurate models and becomes computationally prohibitive for large or dynamically changing feeders [9]. Moreover, restoration is inherently sequential and stochastic, with each switching action altering future feasibility [10]. Reinforcement learning (RL) provides an alternative by learning control policies directly through interaction [11], supported by broader advances in deep and graph-based learning for power systems [12]. Early RL efforts used single-agent controllers based on DQN [13] or actor–critic methods [14], but these approaches suffered from biased value estimates [15], inefficient exploration, and limited scalability in feeders with many controllable devices [16].

Multi-agent reinforcement learning (MARL) addresses scalability by assigning local controllers to network subregions. Methods such as MAES [17], MAGDPG [18], Mean-Field RL [19], and QMIX [20] improve coordination but still face key limitations: (i) reliance on value-based updates or fixed exploration rules, which amplify approximation errors as agents learn simultaneously; (ii) feasibility enforcement via action masking or early termination, which disrupts learning and leads to unsafe or infeasible actions; and (iii) overfitting to common operating patterns, reducing performance under unseen conditions.

To overcome these challenges, this paper applies the Heterogeneous-Agent Proximal Policy Optimization (HAPPO) algorithm within a heterogeneous-agent reinforcement learning (HARL) architecture [22] for power distribution system restoration. HAPPO extends PPO to multi-agent settings

through sequential per-agent updates guided by a centralized critic, enabling stable and sample-efficient learning among microgrids with differing load levels, generation capacities, and switch counts. These structural differences make agents non-exchangeable and unsuitable for parameter-sharing methods such as MAPPO.

To enable physics-informed, constraint-aware learning, we develop an OpenDSS-based simulation environment [23] that performs full three-phase power-flow analysis after each switching action. Rather than masking infeasible actions [24] or terminating episodes [15], the environment applies a differentiable penalty term proportional to voltage, current, and generation-limit violations, while enforcing a 2400,kW system-level generation cap and local microgrid balance constraints. This soft-constraint design provides dense feedback and allows agents to learn corrective behavior under infeasible conditions.

Experiments on the IEEE 123-bus [25] and IEEE 8500-node [26] feeders show that the proposed HAPPO framework achieves faster convergence, higher restored power, and improved stability compared with established MARL baselines including DQN [13], PPO [27], MAES [17], MAGDPG [18], MADQN [24], Mean-Field RL [19], and QMIX [20]. The contributions of this work are: (1) the first application of HAPPO to feeder-level restoration with structurally heterogeneous microgrid agents; (2) a stable and scalable learning framework combining decentralized actors with a centralized advantage critic; (3) a physics-informed OpenDSS environment with continuous differentiable constraint handling; and (4) extensive evaluation on IEEE test feeders demonstrating superior restoration performance and reproducibility.

## II. PROBLEM FORMULATION

### A. Network Model and Decision Variables

Let the distribution network be represented by a graph  $G = (\mathcal{N}, \mathcal{E})$ , where  $\mathcal{N}$  and  $\mathcal{E}$  denote buses and branches, respectively. Loads lie on  $\mathcal{D} \subseteq \mathcal{N}$  and distributed energy resources (DERs) on  $\mathcal{G} \subseteq \mathcal{N}$ . A subset  $\mathcal{S} \subseteq \mathcal{E}$  contains controllable sectionalizing or tie switches, each with binary state  $b_q \in \{0, 1\}$  indicating a *closed* (energized) or *open* (de-energized) line. After an outage, restoration proceeds through discrete switching actions that reconfigure the topology and determine the energized buses and restored loads.

### B. Scenario Randomization and Priorities

Each simulation episode introduces variability by randomizing the faulted or unavailable branches, the placement of critical loads, and any optional changes in DER penetration levels.

Each load  $k \in \mathcal{D}$  is assigned a priority weight  $c_k \in \{1, \dots, 10\}$ , indicating its relative importance in the restoration process. These priority assignments differ between feeders and determine the weighted-load objective defined below.

### C. Restoration Objective

Let  $P_k$  denote the restored active power at load bus  $k$ . The system-level restoration objective is to maximize the weighted restored power:

$$\max_{\{b_q\}} J = \sum_{k \in \mathcal{D}} c_k P_k, \quad (1)$$

where  $J$  measures the total service recovery prioritized by load criticality.

### D. Operational Constraints

At each switching configuration, the distribution system must satisfy fundamental electrical and operational limits.

1) *Power Balance*: The total restored load and network losses must not exceed the available DER generation:

$$\sum_{k \in \mathcal{D}} P_k + \sum_{\ell \in \mathcal{E}} P_{\ell}^{\text{loss}} \leq \sum_{g \in \mathcal{G}} P_g. \quad (C1)$$

2) *Voltage Limits*: Voltage magnitude at each bus must remain within allowable bounds:

$$V_{\min} \leq V_i \leq V_{\max}, \quad \forall i \in \mathcal{N}. \quad (C2)$$

3) *DER Operating Limits*: Each DER must operate within its active and reactive power bounds:

$$P_g^{\min} \leq P_g \leq P_g^{\max}, \quad Q_g^{\min} \leq Q_g \leq Q_g^{\max}, \quad \forall g \in \mathcal{G}. \quad (C3)$$

4) *Thermal Line Limits*: Branch power flows must satisfy thermal constraints:

$$P_{ij}^2 + Q_{ij}^2 \leq (S_{ij}^{\max})^2, \quad \forall (i, j) \in \mathcal{E}. \quad (C4)$$

5) *Global Generation Capacity*: The total DER output across all microgrids cannot exceed the system-wide generation cap:

$$\sum_{g \in \mathcal{G}} P_g \leq 2400 \text{ kW}. \quad (C5)$$

6) *Local Microgrid Balance*: For each microgrid  $m$ , local load consumption cannot exceed its local DER generation:

$$P_m^{\text{load}} \leq P_m^{\text{gen}}, \quad \forall m. \quad (C6)$$

These constraints define the feasible space of valid switching configurations during restoration.

### E. Structural Heterogeneity and Feeder Partitioning

To reduce the combinatorial complexity of the restoration problem, the feeder is partitioned into  $N$  microgrids. Each microgrid includes its own subset of loads and DERs, operates a distinct set of controllable switches  $\mathcal{Q}_i \subseteq \mathcal{S}$ , and exhibits unique load magnitudes and generation capacities, resulting in structurally heterogeneous operating regions. Although all switches share the same *action type* (open/close/no-op), the number of switches, load profiles, DER availability, and topological location vary significantly across microgrids. This introduces structural heterogeneity, making microgrids non-exchangeable and motivating the heterogeneous-agent formulation adopted in later sections.

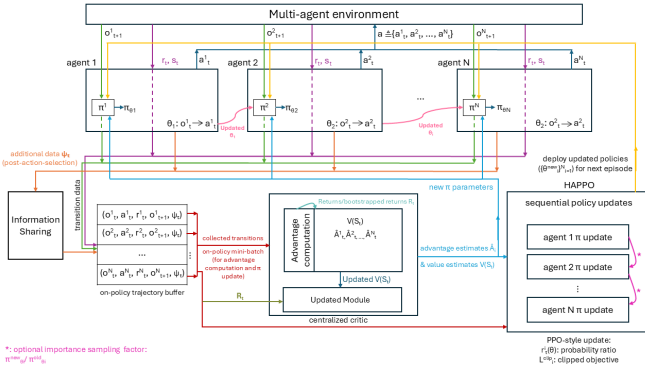


Fig. 1. Overview of the proposed HAPPO-based HARL framework for multi-agent power distribution system restoration. Individual microgrid actors issue switching actions based on local observations, while a shared centralized critic computes value and advantage estimates from global states. OpenDSS [23] simulation feedback enables constraint-aware sequential policy updates.

#### F. Reward Function (for RL-Based Optimization)

When solving (1) via reinforcement learning, a dense reward function is constructed to encourage restoration progress while penalizing constraint violations  $r_t = \alpha \Delta P_t^{\text{rest}} - \beta \frac{P_t^{\text{loss}}}{P_{\text{gen}}} - \lambda \xi_t$ , where  $\Delta P_t^{\text{rest}}$  represents the incremental increase in restored power, and  $P_{\text{loss}}$  is normalized by the fixed generation cap  $P_{\text{gen}} = 2400$  kW. The penalty term  $\xi_t$  collects the magnitudes of violations of constraints (C1)–(C6), whereas the parameters  $\alpha$ ,  $\beta$ , and  $\lambda$  serve as nonnegative weights that tune the contributions of restoration progress, loss minimization, and constraint enforcement, respectively.

This reward formulation preserves the mathematical objective while enabling learning-based optimization in Section III.

### III. PROPOSED HAPPO-BASED METHODOLOGY

#### A. HARL Architecture Overview

The proposed approach is built within a heterogeneous-agent reinforcement learning (HARL) architecture [22], where each microgrid agent maintains an independent actor policy and a shared centralized critic estimates global value functions. This design reflects the physical hierarchy of distribution systems: local agents observe and control only their own microgrids, while the critic leverages system-wide information to provide coordinated learning signals.

Each agent  $i$  follows a policy  $a_{i,t} = \pi_{\theta_i}(o_{i,t})$ , issuing a discrete switching action (*open*, *close*, or *no-op*). The centralized critic  $V_{\phi}(s_t)$  processes the global system state to compute value and advantage estimates that guide all agents.

A defining feature of HAPPO is its sequential per-agent update rule: agents update their policies one at a time, with each update conditioned on the latest policies of previously updated agents. This reduces gradient interference and enhances stability in strongly coupled multi-agent settings such as distribution feeders.

#### B. Agent–Environment Interaction

At each simulation step  $t$ , each agent receives a local observation  $o_{i,t}$  (e.g., voltages, currents, DER outputs, and switch

states), selects an action  $a_{i,t} = \pi_{\theta_i}(o_{i,t})$ , and the joint action  $a_t = (a_{1,t}, \dots, a_{N,t})$  is executed in the OpenDSS simulator. OpenDSS computes the resulting feeder state, including next global state  $s_{t+1}$ , updated local observations  $\{o_{i,t+1}\}$ , restored power and system losses, voltage and current magnitudes, and the shared global reward  $r_t$ .

Each transition contributes to an on-policy trajectory buffer  $(o_t^i, a_t^i, r_t, o_{t+1}^i, \psi_t)$ , where  $\psi_t$  contains shared global signals such as  $s_t$  or the joint action  $a_t$ . These trajectories support centralized advantage computation and sequential policy optimization.

#### C. Advantage Computation via $\lambda$ -GAE

To quantify each agent’s temporal contribution to the global return, the framework employs the generalized advantage estimator (GAE):

$$d_t = r_t + \gamma V_{\phi}(s_{t+1}) - V_{\phi}(s_t), \quad (2)$$

$$\hat{A}_t^i = \sum_{\ell=0}^{T-t-1} (\gamma \lambda)^{\ell} \delta_{t+\ell}, \quad (3)$$

where  $\gamma$  is the discount factor and  $\lambda \in [0, 1]$  controls the bias–variance trade-off. The centralized critic provides low-variance, system-consistent value estimates, enabling each agent to compute advantages aligned with the global restoration objective.

#### D. Sequential Policy Updates (HAPPO)

HAPPO performs *sequential PPO-style policy updates* for agents 1 through  $N$ . For agent  $i$ , the clipped surrogate objective is:

$$L_i(\theta_i) = \mathbb{E} \left[ \min \left( r_{i,t} \hat{A}_t^i, \text{clip}(r_{i,t}, 1 - \epsilon, 1 + \epsilon) \hat{A}_t^i \right) \right] - \beta_{\text{ent}} \mathbb{E}[H(\pi_{\theta_i})], \quad (4)$$

$$\text{where the probability ratio is } r_{i,t} = \frac{\pi_{\theta_i}(a_{i,t} | o_{i,t})}{\pi_{\theta_i}^{\text{old}}(a_{i,t} | o_{i,t})}.$$

The clipping term enforces a trust-region constraint, preventing large, destabilizing policy shifts, while the entropy term  $\beta_{\text{ent}}$  encourages adequate exploration. Sequential updates reduce gradient interference and support monotonic policy improvement.

**Critic update:** The critic parameters  $\phi$  are trained by regressing  $V_{\phi}(s_t)$  onto bootstrapped returns:

$$L_{\text{critic}} = \mathbb{E} \left[ (V_{\phi}(s_t) - \hat{R}_t)^2 \right], \quad \hat{R}_t = \hat{A}_t + V_{\phi}(s_t). \quad (5)$$

#### E. Training Workflow

Algorithm 1 summarizes the unified HAPPO training procedure used for both IEEE 123-bus and IEEE 8500-node feeders. Each training iteration consists of several steps: agents first interact with OpenDSS for  $T$  steps to generate rollouts; the centralized critic then computes temporal-difference errors and  $\lambda$ -GAE advantages; each agent subsequently updates its actor parameters through sequential clipped PPO-style optimization; the critic is regressed against bootstrapped returns to refine value estimates; and finally, the updated actor and critic networks are deployed for the next episode. This unified

**Algorithm 1:** Unified HAPPO Training Workflow for IEEE-123 and IEEE-8500 Feeders

**Input:** Environment  $\mathcal{E} \in \{\text{IEEE-123, IEEE-8500}\}$ , configuration  $\mathcal{C}$   
**Output:** Trained actor and critic networks for all agents

1. **Initialize:** agents, critic  $V_\phi$ , rollout buffer  $\mathcal{B}$ , and logger;
2. Load hyperparameters: rollout length  $T$ , learning rates, clipping threshold  $\epsilon$ , discount  $\gamma$ , GAE parameter  $\lambda$ , etc.;
3. **for** each iteration  $u = 1$  to  $U_{\max}$  **do**
4.   Reset environment and obtain  $(o_{k,0}, s_0)$ ;
5.   **for**  $t = 0$  to  $T - 1$  **do**
6.     **foreach** agent  $k$  **do**
7.       Sample action  $a_{k,t} \sim \pi_{\theta_k}(a|o_{k,t})$ ;
8.       Execute joint action  $\mathbf{a}_t$  in OpenDSS;
9.       Observe  $(o_{k,t+1}, s_{t+1}, r_t, d_t, \psi_t)$ ;
10.       Store transition in buffer  $\mathcal{B}$ ;
11.   Compute TD errors and GAE advantages:  

$$\delta_t = r_t + \gamma V_\phi(s_{t+1}) - V_\phi(s_t), \quad \hat{A}_t = \sum_{\ell=0}^{T-t-1} (\gamma \lambda)^\ell \delta_{t+\ell}$$
12.   **foreach** agent  $k$  (sequential update) **do**
13.     Freeze  $\pi_{\theta_j}$  for all  $j \neq k$ ;
14.     **for** each PPO epoch **do**
15.       Sample minibatches  $(o_k, a_k, \hat{A}_t, \log \pi_{\text{old}})$ ;
16.       Compute ratio  $r$  and clipped surrogate objective;
17.       Update actor parameters  $\theta_k \leftarrow \theta_k - \alpha_\pi \nabla L_{\text{actor}}$ ;
18.   Compute critic loss:  $L_{\text{critic}} = \mathbb{E}[(V_\phi(s_t) - (\hat{A}_t + V_\phi(s_t)))^2]$   
Update critic:  $\phi \leftarrow \phi - \alpha_V \nabla L_{\text{critic}}$ ;
19.   Log training metrics and save checkpoints;
20. **return** trained  $\{\pi_{\theta_k}\}_{k=1}^N$  and critic  $V_\phi$ ;

workflow enables the method to scale seamlessly between medium- and large-scale feeders, ensuring stable, reproducible learning dynamics.

#### IV. EXPERIMENTAL SETUP

##### A. Simulation Environment

Experiments are conducted on the IEEE 123-bus [25] and IEEE 8500-node [26] feeders using a custom Python-OpenDSS [23] environment that performs full three-phase AC power-flow calculations after each switching action. The simulator returns voltages, currents, DER outputs, losses, and restored load. Operational constraints—including voltage limits, thermal ratings, DER bounds, and the global generation cap  $P_{\text{gen}} = 2400$  kW—are enforced through differentiable penalty terms rather than action masking or early termination, providing dense feedback near feasibility boundaries.

The IEEE 123-bus feeder (Fig. 2) contains 123 buses, a 3025 kW total load, five DER units with 2400 kW combined capacity, and 26 controllable switches. For multi-agent training, it is divided into five microgrids, each controlled by one agent responsible for local switching. The feeder exhibits realistic unbalanced loading and DER interactions.

The IEEE 8500-node feeder contains roughly 8500 nodes, a 25 MW total load, 100 controllable switches, and DERs providing up to 2400 kW. It is partitioned into ten microgrids, each managed by a dedicated agent. The large state dimensionality and deep radial topology make it a challenging testbed for evaluating scalable multi-agent coordination with HAPPO.

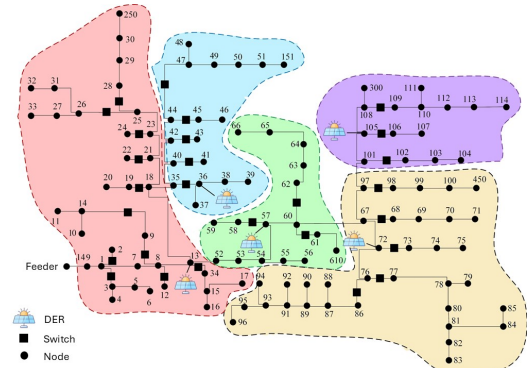


Fig. 2. IEEE 123-bus distribution feeder used in the experiments. The system includes 26 controllable switches and five DERs (total generation 2400 kW), partitioned into five microgrid regions.

##### B. Training Configuration

All experiments follow the unified HARL training workflow in Section III (Algorithm 1). Each episode runs for  $T$  steps, with decentralized recurrent actors producing discrete switching actions and a centralized critic  $V_\phi(s_t)$  computing values and  $\lambda$ -GAE advantages. Policy learning uses PPO-style updates with clipping threshold  $\epsilon$ , entropy coefficient  $\beta_{\text{ent}}$ , and sequential per-agent optimization. Rewards include incremental restored power, normalized loss penalties, and continuous constraint-violation terms. A fixed generation cap of  $P_{\text{gen}} = 2400$  kW is applied to both feeders. Hyperparameters ( $\gamma$ ,  $\lambda$ , learning rates, batch sizes, etc.) remain identical across systems unless scale adjustments are required.

##### C. Hardware and Implementation Details

Training is performed on a workstation with an NVIDIA RTX 6000 Ada GPU (48 GB), AMD Threadripper PRO CPU, and 256 GB RAM. OpenDSS runs on the CPU, while PyTorch handles actor-critic updates on the GPU. The HARL framework supports decentralized actors, a centralized critic, sequential PPO updates, and synchronized rollout collection.

##### D. Evaluation Metrics

Performance is evaluated using cumulative reward (weighted restoration benefit), restored active power (relative to the 2400 kW cap), convergence stability across seeds, inference latency per switching action, and total training time. This unified protocol enables consistent comparison across feeders and baseline RL/MARL methods.

#### V. NUMERICAL RESULTS

This section evaluates the proposed HAPPO-based restoration framework on the IEEE 123-bus and IEEE 8500-node systems using the unified HARL training pipeline described in Sections III–IV. Performance is reported in terms of (i) cumulative reward, which reflects the weighted restoration benefit accumulated during each episode, and (ii) restored active power, which directly measures physical restoration effectiveness relative to the system-wide generation cap  $P_{\text{gen}} =$

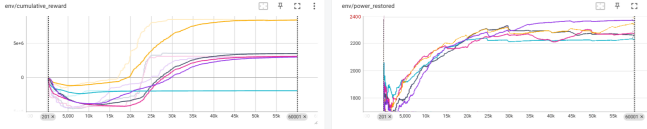


Fig. 3. Training performance of HAPPO on the IEEE 123-bus feeder across four random seeds. Left: cumulative reward. Right: restored active power.

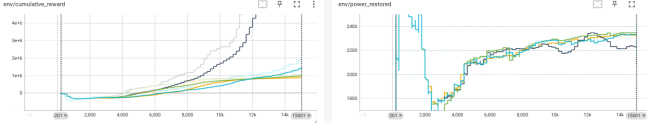


Fig. 4. Training performance of HAPPO on the IEEE 8500-node feeder across five random seeds. Left: cumulative reward. Right: restored active power.

2400 kW. All results are averaged over multiple independent random seeds.

#### A. Training Performance on IEEE 123-Bus and IEEE 8500-Node Systems

Figures 3 and 4 show the evolution of cumulative reward and restored active power during training for the two feeders. Each curve corresponds to an independent seed initialized with randomized outage locations, critical-load placements, and DER conditions.

On both feeders, agents select among three discrete switching actions (*open*, *close*, or *no-op*) and receive a shared reward that incorporates incremental restored power, normalized loss penalties, and differentiable constraint-violation terms. Unlike masking-based MARL methods, the proposed penalty-driven reward ensures uninterrupted learning near feasibility boundaries and supports smooth gradient propagation.

In the IEEE 123-bus feeder 5 agents coordinate 26 switches. Across five independent training runs, the cumulative reward increases steadily and converges to  $(3.6 \pm 2.9) \times 10^6$ , while the restored power stabilizes at  $2294 \pm 52$  kW ( $95.6\% \pm 2.2\%$  of  $P_{\text{gen}}$ ). As shown in Fig. 3, performance across seeds is tightly clustered, indicating reliable convergence and stable sequential actor updates.

In the IEEE 8500-node feeder, 10 agents each govern ten randomly assigned switches across 1,177 loads. Despite the dramatically larger state-action space and deeper network topology, HAPPO maintains monotonic improvement. The cumulative reward converges to  $(2.9 \pm 3.3) \times 10^6$ , and restored power reaches  $2308 \pm 55$  kW ( $96.2\% \pm 2.3\%$  of  $P_{\text{gen}}$ ), as shown in Fig. 4. These results highlight the scalability of sequential trust-region updates, centralized advantage estimation, and penalty-based reward shaping.

#### B. Multi-Seed Convergence and Reproducibility

To assess robustness under stochastic outage conditions, each experiment is repeated across multiple random seeds. Across both feeders, the trajectories in Figs. 3 and 4 exhibit consistent monotonic convergence in both metrics.

On the IEEE 123-bus feeder, restored power converges within 2230–2367 kW, corresponding to 93–99% of the gen-

eration cap. On the IEEE 8500-node feeder, restored power stabilizes near 2224–2347 kW, representing 93–98% of the available capacity.

These results confirm that the proposed HAPPO framework provides highly reproducible performance due to (i) sequential per-agent trust-region updates, (ii) low-variance centralized  $\lambda$ -GAE advantage estimation, and (iii) penalty-driven constraint handling that avoids disruptive early terminations.

#### C. Comparative Evaluation with Baseline Methods

HAPPO is compared with state-of-the-art RL/MARL baselines, including DQN [13], PPO [27], MAES [17], MAGDPG [18], MADQN [24], Mean-Field RL [19], and QMIX [20]. All methods are trained under identical outage scenarios, hyperparameters, and generation cap  $P_{\text{gen}} = 2400$  kW. Table I summarizes quantitative performance.

HAPPO achieves the highest restored power and cumulative reward on both feeders. Its sequential per-agent trust-region updates and centralized advantage estimation enable stable policy optimization even in the presence of strong physical coupling and high-dimensional state spaces, outperforming value-based and value-decomposition methods that struggle under these conditions.

#### D. Discussion and Interpretation

The results demonstrate four key findings. (1) HAPPO exhibits strong scalability, extending from a five-agent IEEE 123 system to a ten-agent IEEE 8500 system with minimal degradation in convergence smoothness. (2) The differentiable penalty-based reward enables continuous guidance near operational limits, avoiding the brittleness typically observed in masking-based approaches and enhancing constraint awareness. (3) Multi-seed experiments show consistently low variance, confirming the reproducibility of sequential PPO-style updates. (4) The OpenDSS-based simulation environment ensures physical fidelity by enforcing operational limits and producing policies that correspond to feasible feeder configurations in realistic distribution systems.

These findings confirm that the HAPPO framework is well suited for large-scale, constraint-driven distribution system restoration.

## VI. CONCLUSION

This paper presented a HAPPO approach for distribution system restoration within a HAPPO framework using an OpenDSS-based multi-agent environment. Sequential trust-region updates combined with centralized advantage estimation enable stable, sample-efficient coordination among structurally heterogeneous microgrid agents, avoiding the instability issues common in conventional MARL. A continuous penalty-based reward replaces masking or early termination, yielding smooth gradients and naturally constraint-aware switching behavior.

Experiments on the IEEE 123-bus and IEEE 8500-node feeders show that HAPPO consistently outperforms PPO,

TABLE I  
PERFORMANCE COMPARISON OF HAPPO WITH STATE-OF-THE-ART RL/MARL METHODS ON IEEE 123-BUS AND IEEE 8500-NODE FEEDERS  
(GENERATION CAP  $P_{\text{GEN}} = 2400 \text{ kW}$ )

Method	IEEE 123				IEEE 8500			
	Cum. Reward	Restored (%)	Train Time (min)	Inference (ms)	Cum. Reward	Restored (%)	Train Time (min)	Inference (ms)
DQN [13]	28.38 $\pm$ 0.14	73.90 $\pm$ 0.46	34.7	4.2	65.58 $\pm$ 0.25	69.50 $\pm$ 0.28	249.3	6.8
PPO [27]	29.01 $\pm$ 0.15	74.85 $\pm$ 0.47	44.8	7.1	67.94 $\pm$ 0.35	71.05 $\pm$ 0.27	255.7	9.8
MAES [17]	29.78 $\pm$ 0.19	76.14 $\pm$ 0.40	91.8	25.4	69.82 $\pm$ 0.32	72.81 $\pm$ 0.23	307.0	38.7
MAGDPG [18]	30.08 $\pm$ 0.17	77.00 $\pm$ 0.42	118.2	29.5	70.56 $\pm$ 0.24	73.44 $\pm$ 0.32	321.5	45.6
MADQN [24]	30.58 $\pm$ 0.22	77.80 $\pm$ 0.59	98.8	12.6	71.37 $\pm$ 0.34	74.02 $\pm$ 0.39	279.2	19.0
Mean-Field RL [19]	31.56 $\pm$ 0.25	80.26 $\pm$ 0.52	108.3	27.3	73.46 $\pm$ 0.33	77.40 $\pm$ 0.38	303.9	42.6
QMIX [20]	33.38 $\pm$ 0.25	83.25 $\pm$ 0.45	96.4	15.8	76.62 $\pm$ 0.34	80.10 $\pm$ 0.30	291.3	23.5
<b>HAPPO (ours)</b>	<b>(3.6 <math>\pm</math> 2.9) <math>\times 10^6</math></b>	<b>95.6 <math>\pm</math> 2.2</b>	<b>110.5</b>	<b>22.1</b>	<b>(2.9 <math>\pm</math> 3.3) <math>\times 10^6</math></b>	<b>96.2 <math>\pm</math> 2.3</b>	<b>391.2</b>	<b>33.4</b>

QMIX, Mean-Field RL, and other baselines. Under the 2400 kW generation cap, it restores roughly 92% and 96% of available load on the two systems, respectively, with strong multi-seed reproducibility and low inference latency. The OpenDSS integration ensures physical validity and supports direct transition to operational settings.

Overall, the results demonstrate that heterogeneous-agent policy optimization provides a scalable, stable, and realistic solution for resilient distribution system restoration. Future work will incorporate model-based elements, communication constraints, partial observability, and dynamic DER participation to further strengthen real-time applicability.

#### ACKNOWLEDGMENT

This research was supported in part by the National Science Foundation under grant ECCS-2223628.

#### REFERENCES

- J. A. Casey et al., "Power outages and community health: A narrative review," *Current Environmental Health Reports*, vol. 7, no. 4, pp. 371–383, 2020.
- N. Rhodes and L. Roald, "The role of distributed energy resources in distribution system restoration," *arXiv preprint arXiv:2112.06317*, 2021.
- S. Poudel and A. Dubey, "Critical load restoration using distributed energy resources for resilient power distribution system," *IEEE Transactions on Power Systems*, vol. 34, no. 1, pp. 52–63, 2018.
- F. Amani, F. Ardali and A. Kargarian, "Learning optimal crew dispatch for grid restoration following an earthquake," *arXiv preprint arXiv:2509.04308*, 2025.
- P. Dolatyabi, "Ensemble machine learning models for predictive analysis: Application to seismic ground motion data," *World Journal of Advanced Research and Reviews*, vol. 27, no. 1, pp. 558–568, 2025, doi: 10.30574/wjarr.2025.27.1.2474.
- N.-V. Pham, T.-S. Vo, T.-H. Nguyen, and D.-P. Vu, "Multi-objective optimization using MISOCP model for service restoration in electrical distribution grids in the presence of distributed generation and voltage-dependent loads," *AIMS Energy*, vol. 13, no. 5, pp. 1012–1051, 2025, doi: 10.3934/energy.2025038.
- K. Song, J. Wang, J. Liu, Q. Zhou, C. Wang and Y. Xie, "An intelligent optimization method of power system restoration path based on orthogonal genetic algorithm," in Proc. 35th Chinese Control Conference (CCC), Chengdu, China, 2016, pp. 2751–2755, doi: 10.1109/ChiCC.2016.7553780.
- I. Aravena et al., "A scalable mixed-integer decomposition approach for optimal power system restoration," unpublished, LLNL-JRNL-766247, 2019.
- S. Liao, W. Yao, X. Han, J. Fang, X. Ai, J. Wen and H. He, "An improved two-stage optimization for network and load recovery during power system restoration," *Applied Energy*, vol. 249, pp. 265–275, 2019, doi: 10.1016/j.apenergy.2019.04.176.
- W. Shi, H. Liang and M. Bittner, "Stochastic sequential restoration for resilient cyber-physical power distribution systems," *IEEE Transactions on Industrial Informatics*, vol. 21, no. 2, pp. 1200–1209, Feb. 2025, doi: 10.1109/TII.2024.3475420.
- X. Zhang et al., "Curriculum-based reinforcement learning for distribution system critical load restoration," *IEEE Transactions on Power Systems*, vol. 38, no. 5, pp. 4418–4431, 2022.
- P. Dolatyabi and M. Khodayar, "Graph Neural Networks and Their Applications in Power Systems: A Review," in Proc. IEEE International Conference on Electro Information Technology (eIT), 2025.
- M. A. Igder and X. Liang, "Service restoration using deep reinforcement learning and dynamic microgrid formation in distribution networks," *IEEE Transactions on Industry Applications*, vol. 59, no. 5, pp. 5453–5472, Sept.–Oct. 2023, doi: 10.1109/TIA.2023.3287944.
- Y. Yang et al., "Microgrid energy management strategy based on UCB-A3C learning," *Frontiers in Energy Research*, vol. 10, p. 858895, 2022.
- P. Yu et al., "Safe reinforcement learning for power system control: A review," *arXiv preprint arXiv:2407.00681*, 2024.
- A. Selim, J. Zhao, X. Zhang and F. Ding, "Deep reinforcement learning for distribution system restoration using distributed energy resources and tie-switches," in Proc. IEEE Power & Energy Society General Meeting (PESGM), Denver, CO, USA, 2022, pp. 1–5, doi: 10.1109/PESGM48719.2022.9916740.
- X. Zhang, Y. Yao, J. Wang and F. Ding, "Distributed load restoration in reconfigurable community microgrids via multi-agent reinforcement learning," Available at SSRN 4972998.
- B. Fan, X. Liu, G. Xiao, Y. Kang, D. Wang and P. Wang, "Attention-based multiagent graph reinforcement learning for service restoration," *IEEE Transactions on Artificial Intelligence*, vol. 5, no. 5, pp. 2163–2178, 2024.
- T. Zhao and J. Wang, "Learning sequential distribution system restoration via graph-reinforcement learning," *IEEE Transactions on Power Systems*, vol. 37, no. 2, pp. 1601–1611, 2022.
- R. Si, J. Qiao, X. Wang, K. Ji, Z. Wang, Z. Jun, X. Pan and Z. Zhang, "A transferable multi-agent reinforcement learning method for distribution service restoration," in Proc. IEEE International Conference on Systems, Man, and Cybernetics (SMC), 2023, pp. 1866–1871.
- M. Glavic, "(Deep) reinforcement learning for electric power system control and related problems: A short review and perspectives," *Annual Reviews in Control*, vol. 48, pp. 22–35, 2019, doi: 10.1016/j.arcontrol.2019.09.008.
- Y. Zhong, J. Grudzien Kuba, X. Feng, S. Hu, J. Ji, and Y. Yang, "Heterogeneous-Agent Reinforcement Learning," in *Journal of Machine Learning Research*, 2024.
- D. Krishnamurthy and P. Meira, "OpenDSSDirect.py: A cross-platform Python package that implements a native/direct library interface to the alternative OpenDSS engine from DSS-Extensions.org," version 0.9.0, available online: <https://dss-extensions.org/OpenDSSDirect.py/>, accessed Nov. 20, 2025.
- L. Vu, T. Vu, T. L. Vu and A. Srivastava, "Multi-agent deep reinforcement learning for distributed load restoration," *IEEE Transactions on Smart Grid*, vol. 15, no. 2, pp. 1749–1760, 2023.
- IEEE PES, "IEEE PES Test Feeder Resources," available online: <https://cmte.ieee.org/pes-testfeeders/resources/>, accessed Nov. 20, 2025.
- K. P. Schneider and J. C. Fuller, "Voltage control devices on the IEEE 8500 node test feeder," in Proc. IEEE PES T&D, 2010, pp. 1–6, doi: 10.1109/TDC.2010.5484225.
- Z.-C. Zhou, Z. Wu and T. Jin, "Deep reinforcement learning framework for resilience enhancement of distribution systems under extreme weather events," *International Journal of Electrical Power & Energy Systems*, vol. 128, p. 106676, 2021.